Measurements of Hadronic, Semileptonic and Leptonic Decays of D Mesons at E_{cm}=3.77 GeV in CLEO-c

Steven R. Blusk
Syracuse University, Department of Physics, 201 Physics Building, Syracuse, NY USA

We report on recent measurements of hadronic, semileptonic and leptonic D decays taken using $\sim$57 pb^{-1} of data collected on the ψ'' resonance using the CLEO-c detector.

1 Introduction

Study of D meson decays provides a laboratory in which to study both the strong and weak interactions. On the ψ'' resonance, $D\bar{D}$ pairs are produced in a pure $J^{PC} = 1^{--}$ state with no additional particles, leading to a powerful kinematic constraint: $E_D = E_{beam}$. Combining this constraint with the excellent hermiticity and particle identification of the CLEO-c detector [1], allows for clean measurements in D decays which have traditionally been statistically limited, difficult or inaccessible.

The analyses presented here include about 57 pb^{-1} of data collected on the ψ'' resonance using the CLEO-c detector. They all proceed by fully reconstructing one D meson in an event (hereafter, referred to a $D_{\rm tag}$), and studying the decay of the second ($D_{\rm sig}$). Tagged samples with excellent signal-to-background (S:B) ratios are achieved by requiring that the energy of the D candidate is consistent with the beam energy. One then can then obtain a mass resolution of order 2 MeV by replacing the D energy with the beam energy, resulting in S:B ratios in Cabibbo-favored modes ranging from $\sim$200:1 to $\sim$5:1. Throughout this paper, charge conjugate modes are implied.

2 Hadronic D Decays

Precise measurement of hadronic D decays are of great importance since, for example, they are often used to normalize B and D semileptonic branching fractions, which in turn are used to

extract CKM matrix elements [2]. The hadronic analysis reconstructs single-tagged and double-tagged events, where one or both D mesons decay into $D^0 \to K^-\pi^+$, $K^-\pi^+\pi^0$, $K^-\pi^+\pi^+\pi^-$ or $D^+ \to K^-\pi^+\pi^+$, $K^-\pi^+\pi^+\pi^0$, $K^0_s\pi^+$, $K^0_s\pi^+\pi^0$, $K^0_s\pi^+\pi^+\pi^-$, $K^+K^-\pi^+$. It is straightforward to show that the individual branching fractions are given by $\mathcal{B}_i = \frac{N_{ij}}{N_j}\frac{\epsilon_j}{\epsilon_{ij}}$ and the number of $D\bar{D}$ pairs by $N_{D\bar{D}} = \frac{N_i N_j}{2N_{ij}}\frac{\epsilon_{ij}}{\epsilon_i\epsilon_j}$, where N_{ij} is the yield of double-tagged events with tag mode j and signal mode i, N_j is the yield of single-tagged events in mode j, and ϵ_{ij}, ϵ_j are their respective reconstruction efficiencies. As $\epsilon_{ij} \approx \epsilon_i\epsilon_j$, the measured $\mathcal{B}_i$'s are nearly independent of the tag modes' efficiencies and almost all reconstruction systematics cancel in $N_{D\bar{D}}$. The 9 $\mathcal{B}_i$'s, $N_{D^0\bar{D}^0}$, and $N_{D^+D^-}$ are extracted through a χ^2 minimization involving the difference between the expected background-subtracted, efficiency-corrected single and double-tagged yields and the corresponding observed yields. The average single tag yields, their efficiencies and the corresponding branching fractions are shown in Table 1. The fitted number of $D^0\bar{D}^0$ and D^+D^- pairs are $(2.06 \pm 0.038 \pm 0.02) \times 10^5$ and $(1.56 \pm 0.04 \pm 0.01) \times 10^5$, where the indicated uncertainties are statistical and systematic. These yields correspond to peak cross-sections $\sigma(e^+e^- \to D^0\bar{D}^0) = 3.60 \pm 0.07^{+0.07}_{-0.05}$ nb and $\sigma(e^+e^- \to D^+D^-) = 2.79 \pm 0.07^{+0.10}_{-0.04}$ nb. The systematic uncertainties include particle reconstruction (0.7% per charged particle, 3%/K^0_s, 2%/π^0), particle identification (0.3%/$\pi^\pm$, 0.7%/K$^\pm$), event selection (1.5%), ψ'' natural width (0.6%), final state radiation (0.5% [1.0%] for single [double] tags), resonant substructure (0.4-1.5%), doubly-Cabibbo suppressed interference (0.8%), and signal fitting (0.5%). Further details of this analysis can be found in the references [3].

Table 1: Summary of branching fraction measurements showing the average number of reconstructed single tags, the average reconstruction efficiency, and the branching fraction measurements in D decays.

Mode	$< N_D >$ ($\times 10^3$)	$< \epsilon_D >$ (%)	$\mathcal{B}$ (%)	$\mathcal{B}$(%) PDG [4]
$D^0 \to K^-\pi^+$	5.13±0.07	65.7±0.3	$3.91 \pm 0.08 \pm 0.09$	3.80 ± 0.09
$D^0 \to K^-\pi^+\pi^0$	9.49±0.07	33.2±0.1	$14.94 \pm 0.30 \pm 0.47$	13.0 ± 0.8
$D^0 \to K^-\pi^+\pi^+\pi^-$	7.44±0.07	44.6±0.2	$8.29 \pm 0.17 \pm 0.32$	7.46 ± 0.31
$D^+ \to K^-\pi^+\pi^+$	7.56±0.09	51.7±0.2	$9.52 \pm 0.25 \pm 0.27$	9.2 ± 0.6
$D^+ \to K^-\pi^+\pi^+\pi^0$	2.42±0.07	27.2±0.2	$6.04 \pm 0.18 \pm 0.22$	6.5 ± 1.1
$D^+ \to K^0_s\pi^+$	1.12±0.04	45.6±0.4	$1.55 \pm 0.05 \pm 0.06$	1.41 ± 0.10
$D^+ \to K^0_s\pi^+\pi^0$	2.55±0.07	23.4±0.2	$7.17 \pm 0.21 \pm 0.38$	4.9 ± 1.5
$D^+ \to K^0_s\pi^+\pi^+\pi^-$	1.61±0.06	31.4±0.2	$3.20 \pm 0.11 \pm 0.16$	3.6 ± 0.5
$D^+ \to K^+K^-\pi^+$	0.63±0.03	42.6±0.5	$0.97 \pm 0.04 \pm 0.04$	0.89 ± 0.08

3 Semileptonic Decays

Semileptonic widths for $D \to X_{s(d)}l^+\nu$ directly probe the elements of the CKM matrix. When $J^P(X_{(s,d)}) = 0^-$, the differential width is given by:

$$\frac{d\Gamma(D \to X_{s(d)}l^+\nu)}{dq^2} = \frac{|V_{cs(cd)}|^2 p^3}{24\pi^3} f(q^2), \quad (1)$$

where q^2 is the momentum transfer squared between the D meson and the final state hadron in the D rest frame. While the normalization of the form factor, $f(q^2)$, must be obtained from theory (lattice QCD, for example), CLEO-c can measure its shape and in doing so provide a stringent test of theoretical predictions. Provided theory is able to describe the shape of $f(q^2)$, we then use this tested theory for the normalization, which then permits immediate extraction of V_{cs} and V_{cd}.

The semileptonic analyses use 9 $D^0_{\rm tag}$ and 6 $D^+_{\rm tag}$ modes. For each tagged event, we search for an electron with $p >$200 MeV/c and additional hadrons recoiling against $D_{\rm tag}$. Charged kaons and pions are separated using a combined dE/dx and RICH information, with an efficiency

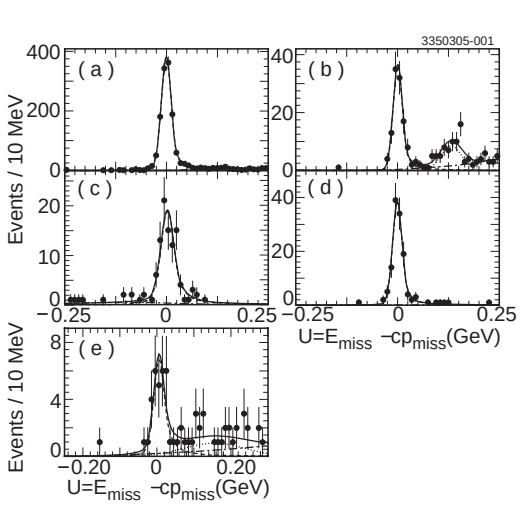

Figure 1: Distributions in $U = E_{miss} - |\vec{p}_{miss}|$ for (a) $D^+ \to K^0_s e^+\nu_e$, (b) $D^+ \to K^{*0}e^+\nu_e$, (c) $D^+ \to \pi^0 e^+\nu_e$, (d) $D^+ \to \rho^0 e^+\nu_e$, and (e) $D^+ \to \omega e^+\nu_e$.

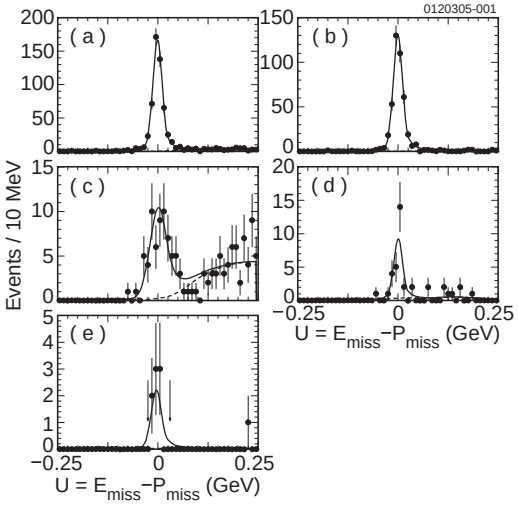

Figure 2: Disributions in $U = E_{miss} - |\vec{p}_{miss}|$ for (a) $D^0 \to K^- e^+\nu_e$, (b) $D^0 \to \pi^- e^+\nu_e$, (c) $D^0 \to K^{*-}[K^-\pi^0]e^+\nu_e$, (d) $D^0 \to K^{*-}[K^0_s\pi^-]e^+\nu_e$, and (e) $D^+ \to \rho^- e^+\nu_e$.

Table 2: Summary of semileptonic branching fraction measurements showing the average reconstruction efficiency, number of reconstructed events, reconstruction efficiency and the branching fractions.

Decay	Yield	ϵ_D (%)	$\mathcal{B}$	$\mathcal{B}$(%) PDG [4]
$D^0 \to K^- e^+\nu_e$	1311.0±36.6	63.6±0.5	$(3.44 \pm 0.10 \pm 0.10)\%$	3.58 ± 0.18
$D^0 \to \pi^- e^+\nu_e$	116.8±11.2	74.2±0.5	$(2.62 \pm 0.25 \pm 0.08) \times 10^{-3}$	0.36 ± 0.06
$D^0 \to K^{*-}[K^-\pi^0]e^+\nu_e$	94.1±10.4	22.0±0.3	$(2.16 \pm 0.24 \pm 0.12)$	
$D^0 \to K^{*-}[K^0_s\pi^-]e^+\nu_e$	125.2±11.6	40.4±0.4	$(2.25 \pm 0.21 \pm 0.13)\%$	3.58 ± 0.18
$D^0 \to K^{*-}e^+\nu_e$			$(2.21 \pm 0.16 \pm 0.09)\%$	2.15 ± 0.35
$D^0 \to \rho^- e^+\nu_e$	31.1±3.3	27.0±0.4	$(1.94 \pm 0.39 \pm 0.13) \times 10^{-3}$	
$D^+ \to K^0_s e^+\nu_e$	545±24	57.1±0.4	$(8.71 \pm 0.38 \pm 0.37)\%$	6.7 ± 0.9
$D^+ \to K^{*0}e^+\nu_e$	422±21	34.8±0.3	$(5.70 \pm 0.28 \pm 0.25)\%$	5.5 ± 0.7
$D^+ \to \pi^0 e^+\nu_e$	63±9	45.2±1.0	$(0.44 \pm 0.06 \pm 0.03)\%$	0.31 ± 0.15
$D^+ \to \rho^0 e^+\nu_e$	27±6	40.0±1.1	$(0.21 \pm 0.04 \pm 0.02)\%$	0.25 ± 0.10
$D^+ \to \omega e^+\nu_e$	8.0±2.8	16.4±0.6	$(0.17 \pm 0.06 \pm 0.01)\%$	

of about 95% and a fake rate of no more than a few percent. Candidate π^0's are formed by pairing two photons and requiring $|M_{\gamma\gamma} - M_{\pi^0}| < 3\sigma$. K^0_s candidates are defined as $\pi^+\pi^-$ pairs which have an invariant mass within 12 MeV/c^2 of the K^0_s mass. Similarly, ρ^0 (ρ^-) candidates are formed by pairing $\pi^+\pi^-$ ($\pi^-\pi^0$) and requiring $|M_{\pi\pi} - M_\rho| < 150$ MeV/c^2. Finally, we reconstruct ω candidates using $\pi^+\pi^-\pi^0$ combinations with $|M_{\pi^+\pi^-\pi^0} - M_\omega| < 20$ MeV/c^2.

For each event, we require that there be no additional charged tracks beyond the $D_{\rm tag}$ and the semileptonic candidate. Properly reconstructed events are identified by a peak at zero in the quantity $U = E_{miss} - |\vec{p}_{miss}|$. Here, E_{miss} and $\vec{p}_{miss}$ are the missing energy and missing momentum in the semileptonic decay, both of which are calculable on an event-by-event basis. The U distributions for $D^+ \to (K^0_S, \bar{K^{*0}}[K^-\pi^+], \pi^0, \rho^0, \omega)e^+\nu_e$ are shown in Figs. 1(a)-(e) respectively. The analogous distributions for $D^0 \to (K^-, \pi^-, K^{*-}[K^-\pi^0], K^{*-}[K^0_s\pi^-], \rho^-)e^+\nu_e$ are shown in Figs. 2(a)-(e), respectively. The $D^+ \to \omega e^+\nu_e$ and $D^0 \to \rho^- e^+\nu_e$ constitute first observations of these decays. The yields, efficiencies and corresponding branching fractions are shown in Table 2. These measurements are already better than world average, and substantially more data are imminent. These analyses will soon be submitted for publication.

4 Leptonic Decays

Leptonic decays of D mesons provide direct access to the decay constant f_D, which is related to the wave-function overlap probability for the constituent c and $\bar{d}$ quarks. An accurate measurement of f_{D^+} provides a stringent test of lattice QCD and other QCD-inspired models to predict decay constants, and in particular, f_B and f_{B_s}.

From a single-tag sample consisting of tagged D^- decays in $K^+\pi^-\pi^-$, $K^+\pi^-\pi^-\pi^0$, $K^0_s\pi^-$, $K^0_s\pi^-\pi^0$, and $K^0_s\pi^+\pi^-\pi^-$, we select a subset of events which contain exactly one extra charged particle. The muon system is not used in this analysis, since most muons in $D^+ \to \mu^+\nu_\mu$ are below its momentum threshold of about 1 GeV. We also require that there is no additional shower with energy exceeding 250 MeV. Signal $D^+ \to \mu^+\nu_\mu$ events are distinguishable by a peak at zero in the missing-mass (MM) spectrum, where $MM^2 = (E_{\rm beam} - E_\mu)^2 - (-p\vec{}_{D^-} - p\vec{}_{\mu^+})^2$ ($=m^2_\nu$, for $D^+ \to \mu^+\nu_\mu$). The distribution in MM^2 for these events is shown in Fig. 3. The large peak at 0.25 GeV^2 is from $D^+ \to K^0_L\pi^+$. The inset shows a blowup of the region near zero, and shows the 8 signal candidates which lie within the signal region, defined to be $\pm 2\sigma$.

The primary sources of background come from $D^+ \to \pi^+\pi^0$ (0.31±0.04 events), where the π^0 is not detected, and $D^+ \to \tau^+\nu_\tau$, followed by $\tau^+ \to \pi^+\nu_\tau$ (0.30±0.07 events). Other backgrounds include $D^+ \to K^0_L\pi^+$ (0.06±0.05 events), $D^0\bar{D}^0$ (0.17±0.17 events) and continuum (0.16±0.16 events). In total, the expected background is 1.00±0.25 events.

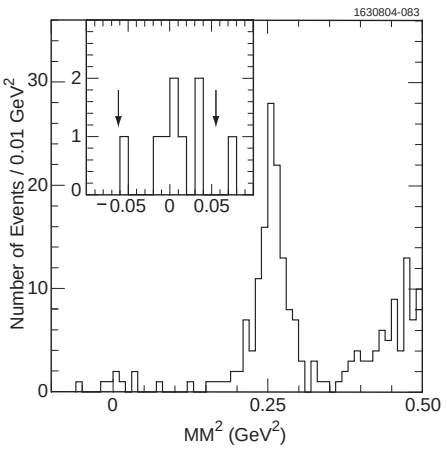

Figure 3: Disributions in MM^2 using D^- tags and one recoiling charged track.

The $D^+ \to \mu^+\nu_\mu$ branching fraction is readily computed using $N_{\rm tag}$=28574±629, $N_{D\to\mu^+\nu_\mu} = 7.0 \pm 2.8$ and a single-muon detection efficiency of (69.9±3.7)%, from which we find $\mathcal{B} = (3.5 \pm 1.4 \pm 1.6) \times 10^{-4}$. Taking $\tau_{D^+} =$ 1.04 ps, and $V_{cd} = 0.224$ [4], we find $f_{D^+} = (202 \pm 41 \pm 17)$ MeV. This is the most precise measurement of this quantity and compares well with lattice QCD and a number of other models. As more data are collected, we will be in a position to discriminate among these predictions. More details can be found in in the references [5].

Acknowledgments

I would like to thank my CLEO colleagues for their input on these analyses. This work was supported by the National Science Foundation and the U.S. Dept. of Energy.

References

1. The CLEO-c detector is an upgrade from the CLEO-III detector in which the silicon detector was replaced with a six-layer vertex drift chamber. For details on the CLEO detector, refer to: CLEO Collaboration, Y. Kubota *et al.,* Nucl. Instrum. Meth. Phys. Res. **A320**, 66 (1992); G. Viehauser *et al.,* Nucl. Instrum. Meth. A**462**, 146 (2001); D. Peterson *et al.,* Nucl. Instrum. Meth. A**478**, 142 (2002); M. Artuso *et al.,* Nucl. Instrum. Meth. A**502**, 91 (2003). The CLEO-c yellow book is available as CLEO Document CLNS-01/1742.
2. M. Kobayashi and T. Maskawa, Prog. Theor. Phys. **49**, 652 (1973).
3. CLEO Collaboration, Q. He *et al.,* Submitted to Phys. Rev. Lett., [hep-ex/0504003].
4. Particle Data Group, S. Eidelman *et al.,* Phys. Lett. **B592**, 1 (2004).
5. CLEO Collaboration, G. Bonvinci *et al.,* Phys. Rev. D **70**, 112004 (2004).